

# Thermal Cutting Temperature Analysis using Probabilistic FEM

Mohd Shahar Sulaiman<sup>1</sup>, Yupiter HP. Manurung<sup>1\*</sup>, M Fadzil<sup>2,3</sup>

<sup>1</sup>Faculty of Mechanical Engineering, UiTM Shah Alam, Malaysia

<sup>2</sup>School of Mechanical Engineering, Universiti Sains Malaysia (Engineering Campus), Nibong Tebal, 14300, Penang, Malaysia,

<sup>3</sup>Centre of Advanced Manufacturing and Material Processing (AMMP Centre), University of Malaya, 50603, Kuala Lumpur, Malaysia.

\*Corresponding author E-mail: [yupiter.manurung@salam.uitm.edu.my](mailto:yupiter.manurung@salam.uitm.edu.my)

## Abstract

This paper investigates the capability of probabilistic FEM to predict temperature distribution due to thermal cutting process. The application of transient heat source causes non-uniform temperature distribution across the parent metal that can lead to non-uniform expansion and contraction during heating and cooling cycle. This phenomenon will induce thermal stresses to the workpiece that can subsequently lead to unwanted cutting deformation. Therefore, forecast of temperature distribution is important in order to control the amount of heat required in the cutting process. The temperature prediction was computed by using non-linear thermo-elastic-plastic numerical analysis with isotropic strain hardening which is also known as deterministic FEM. For comparison, another extension simulation which is probabilistic FEM using Monte Carlo method was carried out by varying the input power. In this study, both simulation methods had been executed by using FEM software MSC MARC. The material used for the simulation was low carbon steel C15 with the thickness of 2 mm. Based on the results obtained, it was found out that slight differences of temperature distributions were predicted between both methods. The small observable differences occurred due to the probabilistic method was only executed to fluctuate the input power, while the other process parameters were still unchanged. Nevertheless, the Monte Carlo method was successfully integrated into the normal simulation which then transforming it into probabilistic analysis. Hence, through probabilistic method, reliability on prediction could be increased in which the prediction would be closer to reality.

**Keywords:** Deterministic FEM, Monte Carlo, MSC MARC, Probabilistic FEM, Thermal Cutting

## 1. Introduction

A heat treatment process, where a metal plate is subjected to a large amount of concentrated heat and the applied part of the metal plate melts or vaporizes away is known as thermal cutting. Thermal cutting is an exothermal process, which means that the burning process maintains itself with less heat required. There are several types of thermal cutting processes such as flame cutting, plasma arc cutting and laser cutting [1]. Plasma arc cutting (PAC) is a cutting method that uses extremely hot plasma gas that melts and partially vaporizes workpiece material. This plasma gas jet is formed by an arc and inert gas flow. Plasma arc is concentrated with a nozzle to produce more precise and even hotter arc, that operates in the region of 10 000 – 14 000 °C. Molten material is removed by the high velocity gas jet, like in oxyfuel gas cutting. Plasma arc is generated by heating gas with an arc. This gas then becomes partially ionized and thus, being able to conduct electricity. Heating the gas rapidly as it travels along the arc causes it to expand. Then the gas is accelerated through the nozzle towards the workpiece. Gases employed in plasma cutting comprise nitrogen, argon, oxygen, air and mixtures of nitrogen/hydrogen and argon/hydrogen [2-3].

Laser cutting is a non-contact thermal cutting process which is a state-of-the-art technology that eliminates such effects as machine vibration, mechanically induced thermal damage and tool wear [4]. It is the most extensively used for producing complex shapes and different geometries with narrow kerf in almost all categories of materials such as metals, non-metals, ceramics and composites. The cutting capability of laser primarily depends on the thermal and

optical properties of the material instead of the mechanical properties [5]. The focused laser beam locally melts the material to be cut and produces a kerf when the molten material is blown away with the aid of assist gas, which flows coaxially with the laser beam. Numerous numerical methods have been applied to perform thermal analysis. In [6], prediction of temperature distribution due to thermal cutting had been carried out on Inconel 718. The finite element analysis was computed based on thermo-mechanical analysis using temperature-dependent material properties. The results showed that the predicted temperature distribution well agreed to the experimental measurement. It was found out that the temperature trend in the specimen with 1 mm thickness was slightly lower than that of specimen with 2 mm thickness. Referring to the explanation in [7], arc-welding process is based on the same principles as arc-cutting process. A welding process normally adds up filler material to the base metal, whereas some materials are removed from the base metal in cutting process. RN Lidam et al. [8] conducted a simulation study on multipassed welding distortion of combined joint types induced by gas metal arc welding (GMAW) process. The simulation had been executed using SYSWELD based on thermo-mechanical-metallurgical analysis.

The plasticity criterion was calculated based on isotropic strain hardening owing to non-cyclic loading in which the mechanical calculations were computed according to metallurgical history primarily following the constitutive equation proposed by Leblond. The outcomes uncovered that the angular distortions predicted using 2D and 3D analyses showed reasonable agreement. It was also found out that 2D analysis required shorter computational time

as compared to 3D analysis. A research on residual stress field induced in pipe girth weld of 316 stainless steel had been carried out by J. G. Mullins et al. [9]. The residual stresses were simulated based on thermo-elastic-plastic mechanical analysis. Three different hardening models had been employed in the finite element analysis comprising isotropic, kinematic and mixed hardening models. The isotropic, kinematic and mixed hardening models were computed according to flow curves at different temperatures, bilinear-Ziegler rule and Lemaitre-Chaboche model respectively. By comparing the simulation results with the experimental verifications, the results revealed that the axial stresses were well predicted by means of isotropic hardening model. In addition, the hoop stresses calculated via isotropic hardening model were also in good agreement with the experimental measurements. The best predictions of hoop stresses were achieved through mixed hardening model. However, the predictions through kinematic hardening model had underestimated both magnitudes of stresses. Even though all criteria have been taken into consideration in numerical simulation, but generally the FEA is deterministic by nature and hence is limited to describe typical characteristics of a system [10]. Different sources of uncertainty come up in the study of complex phenomena such as human error, dynamic loading, inherent randomness of the material and lack of data. The classic FEM has been integrated with other methodologies to develop a novel type of analysis in order to probe the systems with random variations and/or uncertainty in parameters. It has been known as a stochastic finite element method (SFEM) [11], a random finite element method (RFEM) [12] as well as a probabilistic finite element method (PFEM) [13]. Furthermore, to characterize the stochastic nature into a system, random fields are implemented in the classic FEM to describe and establish different stochastic scenarios. The effects of the random variations are evaluated by computing the statistical information of the response variables and evaluating the probability of an outcome of the system. A research on optimization of cutting parameters using probabilistic FEM had been performed by Miloš Madić et al. [14]. In this research, artificial neural network (ANN) based mathematical model using Monte Carlo method was established in order to connect the parameters in CO<sub>2</sub> laser cutting of 304 stainless steel consisting of laser power, cutting speed, assist gas pressure and focus position, as well as kerf taper angle. Monte Carlo method was an approach which manipulating random numbers in simulation algorithm. The Monte Carlo method could be regarded as a general mathematical tool for solving various problems. As compared to experiment, statistical results showed that the kerf taper angle could be calculated through ANN model within good accuracy. The optimum laser cutting parameters which minimized the kerf taper angle could be defined by implementing the Monte Carlo method. It was observed that concentrating the laser beam on around 2/3 of material thickness through low assist gas pressure (9 bar) at combination of high cutting speed (3 m/min) and low laser power (1.6 kW) resulted in acceptable kerf taper angle. By applying the Monte Carlo simulation, the optimization was resolved via the generation of random numbers  $r_{i,j}$  which distributed uniformly in the range between 0 and 1. In order to meet the limitations of the laser cutting parameter values, the random numbers  $r_{i,j}$  were manipulated to produce random numbers  $q_{i,j}$  which uniformly distributed into the range of interest for each of the laser cutting parameter  $[q_i^{min}, q_i^{max}]$ . This was achieved using the following equation:

$$q_{i,j} = q_i^{min} + r_{i,j} \cdot (q_i^{max} - q_i^{min}) \quad (1)$$

## 2. Simulation Method and Procedure

### 2.1 Geometrical Modelling

A schematic illustration of solid FE model used in the simulation is displayed in Figure 1. The dimensions of the model are 100mm x

100mm x 2mm which are referring to the width, length and thickness of the model respectively.

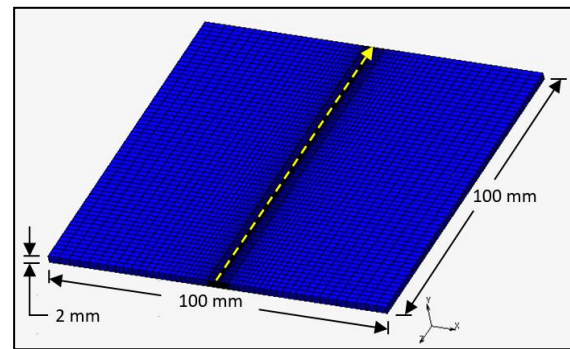


Fig. 1: Geometrical model utilized for simulation

The cutting trajectory is represented by the yellow arrow in which the direction of cutting is determined by the arrow direction. The type of element used for this model is three-dimensional hexahedral element.

### 2.2. Material Modelling

In thermal cutting simulation, low carbon steel material (C15) had been used for analysing the temperature distribution. In simulation, all the computations were executed based on analysis using temperature-dependent material properties as shown in Figure 2 and Figure 3. During cutting process, the workpiece was exposing to high working temperature which could be beyond its melting temperature especially at the focal cutting region and the heat would also be spreading over the heat affected zone (HAZ) area and dissipating into the base metal and the environment. Thus, due to this phenomenon, the magnitudes of values of material properties would change according to the temperature variations. Hence, the temperature-dependent material properties were very important since they would reflect the real situations that occurred to the workpiece during the cutting process.

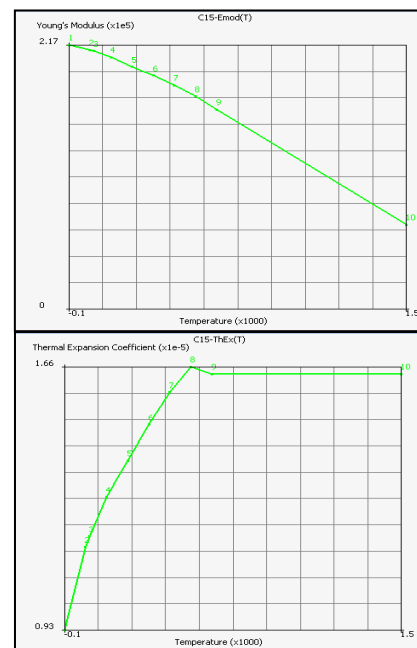


Fig. 2: Temperature-dependent mechanical properties

If the simulation executed using constant material properties, it will merely consider the material behaviour at room temperature which in turn can lead to incorrect prediction. However, the other two material properties which are mass density and Poisson's ratio were

assumed to be  $7850 \text{ kg/m}^3$  and  $0.3$  respectively that were not dependent on temperature.

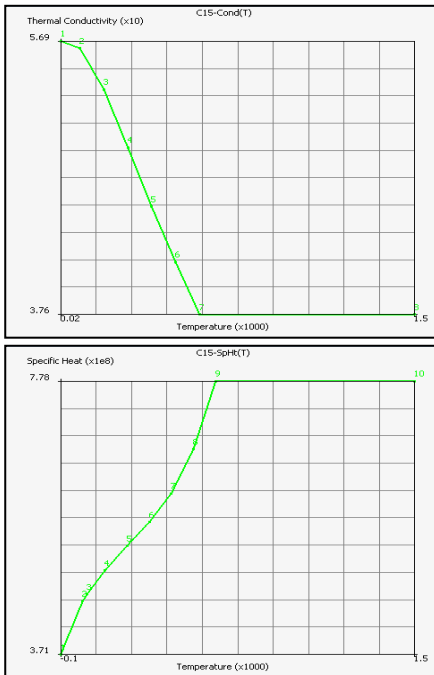


Fig. 3: Temperature-dependent thermo-physical properties

In this study, the temperature analysis was carried out using non-linear thermo-elastic-plastic analysis in which mechanical analysis was also taken into consideration. Based on mechanical analysis, the total deformation was computed through the combination of elastic and plastic strains as expressed by Equation (2).

$$\varepsilon^{total} = \varepsilon^e + \varepsilon^p \quad (2)$$

When the stress in the specimen was below the yield stress of the material, the material behaves elastically and the stress in the specimen was proportional to the strain. However, when the stress in the specimen was greater than the yield stress, the material was no longer exhibiting elastic behaviour and thus, the stress-strain relationship became non-linear. The yield stress of a material is a measured stress level that separates the elastic and plastic behaviour of the material. The magnitudes of the yield stresses were generally obtained from the mechanical properties as defined through the Modulus of Elasticity and flow curve. However, the stresses in a structure are usually multiaxial. A measurement of yielding for the multiaxial state of stress is known as yield condition. In this analysis, for the application of isotropic material, von Mises criterion was selected to describe the yield condition which is commonly used for ductile materials particularly due to its suitability in characterizing metallic behaviour. The von Mises criterion states that yield occurs when the effective (or equivalent) stress,  $\bar{\sigma}$  equals the yield stress,  $\sigma_y$ . The von Mises criterion can be described as expressed by Equation (3), where  $\sigma_1$ ,  $\sigma_2$ , and  $\sigma_3$  are the principal stresses that will be coupled with the strain hardening rule. Figure 4 demonstrates the von Mises yield surface in three-dimensional stress space.

$$\bar{\sigma} = [(\sigma_1 - \sigma_2)^2 + (\sigma_2 - \sigma_3)^2 + (\sigma_3 - \sigma_1)^2]^{1/2}/\sqrt{2} \quad (3)$$

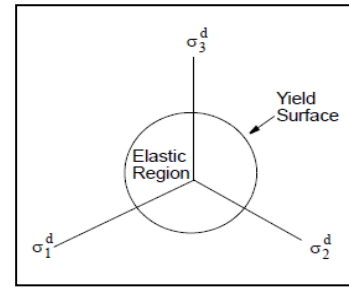


Fig. 4: Three-dimensional stress space

In order to take hardening effects into account, the computational analysis was executed corresponding to the information on material data that characterize the plastic behaviour of the material in the form of flow curves. In addition, these quantities can vary with parameters such as temperature and strain rate. Referring to Figure 5, the slope of the total stress versus plastic strain curve is defined as the workhardening slope ( $H$ ) of the material in which the workhardening slope is a function of plastic strain. Some of the actual data of flow stresses for the material utilized in this simulation were as exhibited in Figure 6. However, there are a lot of flow curves that are not displayed here which were actually used for the analysis such as the flow curves defined at the same strain rates of  $8 \text{ 1/s}$  and  $40 \text{ 1/s}$  with different temperatures ranging between  $20^\circ\text{C}$  and  $1200^\circ\text{C}$ . When it came to a state which was not defined by the available flow curves, the decision was being made through interpolation.

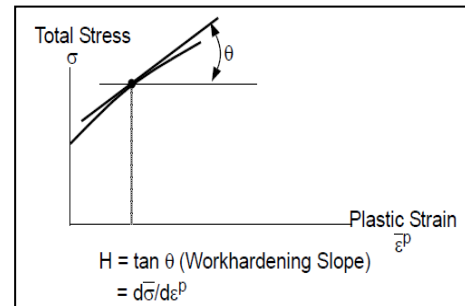


Fig. 5: Definition of workhardening slope

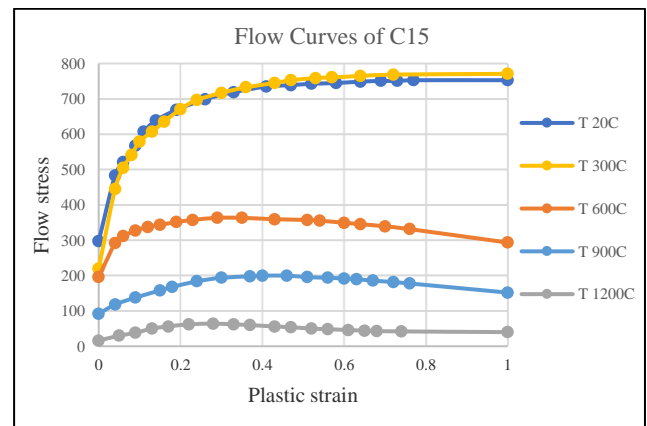


Fig. 6: Flow curves of C15 at the same strain rate of  $1.6 \text{ 1/s}$

### 2.3. Heat Source Modelling

In cutting simulation, one of the most important steps is to model the heat source that can reflect the real process. Suitable heat source model must be selected in accordance with the thermal cutting process. Hence, for the thermal cutting process, a volumetric conical heat source model was employed to replicate the real heat source.

The 3D conical heat source model used in the simulation was defined by C. S. Wu et al. [15] which was obtained through derivation from heat intensity distribution equation of thermal

energy conservation. The Equation (4) was the model equation produced as a result of derivation which could characterize the through thickness decay of heat intensity distribution of the thermal arc. The subsequent Equation (5) was part of the preceding equation which determined the decrease of maximum heat source intensity throughout the thickness of working material. In these equations,  $Q_o$  represents the power input,  $r$  denotes the radial coordinate,  $z$  refers to the z-coordinate and  $r_o$  defines the distribution parameter of the heat intensity. Whereas,  $z_e$  and  $r_e$  represent the z-coordinate and radius of the top surface of the heat source model respectively. Similarly, the z-coordinate and radius of the heat source model at the bottom surface are defined by  $z_i$  and  $r_i$  correspondingly. The configuration of the conical heat source model is illustrated in Figure 7.

$$q(r, z) = \frac{9Q_o e^3}{\pi(e^3 - 1)} \cdot \frac{1}{(z_e - z_i)(r_o^2 + r_e r_i + r_i^2)} \cdot \exp\left(-\frac{3r^2}{r_o^2}\right) \quad (4)$$

$$r_o(z) = r_i + (r_e - r_i) \cdot \frac{z - z_i}{z_e - z_i} \quad (5)$$

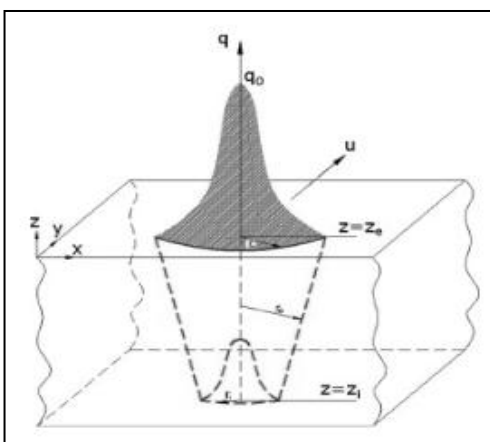


Fig. 7: Conical heat source configuration

### 2.4. Boundary Conditions

There were two types of boundary conditions involved in the cutting simulation consisting of thermal and mechanical boundary conditions. The thermal boundary conditions were defined by heat input of volumetric heat flux as described previously, as well as heat losses due to convection and radiation as expressed by Equation (6) and Equation (7) respectively.

$$q_{conv} = h_{conv}(T_s - T_\infty) \quad (6)$$

$$q_{rad} = \sigma \epsilon (T_s^4 - T_\infty^4) \quad (7)$$

In the above equations,  $h_{conv}$  is convective heat transfer coefficient,  $\sigma$  refers to Stefan Boltzmann's constant and  $\epsilon$  represents thermal emissivity, while  $T_s$  and  $T_\infty$  are surface temperature and ambient temperature respectively. Whereas the mechanical boundary condition was defined by fixation on the model nodes to prevent body motion.

### 2.5. Monte Carlo Simulation

Monte Carlo simulation is a method that takes variability of the inputs into account. The simulation analysis could involve numerous of recalculations before it is complete. Through this method, it could be able to produce distributions of possible outcome values. In this study, to perform the probabilistic analysis, the heat input power of the heat source was fluctuated within a certain range while the other process parameters had been maintained. To ensure it happened, the input power would be varied by using Gaussian random variables. Thus, in order to support this

process, a source of random numbers should be produced. There are a lot of random number generators available, but the most extensively used is linear congruential generator (LCG) which is defined by the following formula [16,17]:

$$x_{i+1} = (a \cdot x_i + c) \text{mod } M, \quad i \geq 0 \quad (8)$$

where  $M$  is the modulus,  $a$  and  $c$  are the multiplier and increment respectively while  $x_o$  is the seed or start value. Through this method, a sequence of pseudo-random integer numbers  $\{x_i\}$  could be generated. Furthermore, in order to produce a random number  $X_i$  in the range between 0 and 1, the random number  $x_i$  generated previously should be divided by  $M$  as shown below:

$$X_i = \frac{x_i}{M}, \quad i \geq 1 \quad (9)$$

However, the random number  $X_i$  produced previously was uniformly distributed,  $U(0,1)$ . For this typical simulation, the Gaussian or normal random variable,  $N(0,1)$  is preferable. Hence, Box-Muller method [18,19,20] could be employed as a tool to transform the uniform random variable into the Gaussian random variable. Through this method, the transformation could be implemented by converting a pair of uniform random variables  $(X_1, X_2)$  into a pair of Gaussian random variables  $(Y_1, Y_2)$  via the subsequent equations:

$$Y_1 = \sqrt{-2\ln(X_1)} \cos(2\pi X_2) \quad (10)$$

$$Y_2 = \sqrt{-2\ln(X_1)} \sin(2\pi X_2) \quad (11)$$

For verification of the probabilistic method, the variation of the input power generated by the algorithm had been computed using general Fortran 77 program. This programming language was employed due to MSC MARC is built based on the same platform. In the cutting simulation, it was executed by using 150 values of different input powers for the variation instead of a single constant value. Therefore, the Fortran program was tested to generate a sequence of 150 random numbers. The program outputs are exhibited in Figure 8. From the red bell curve as shown in the figure, it could be proven that the random input powers were generated according to normal distribution.

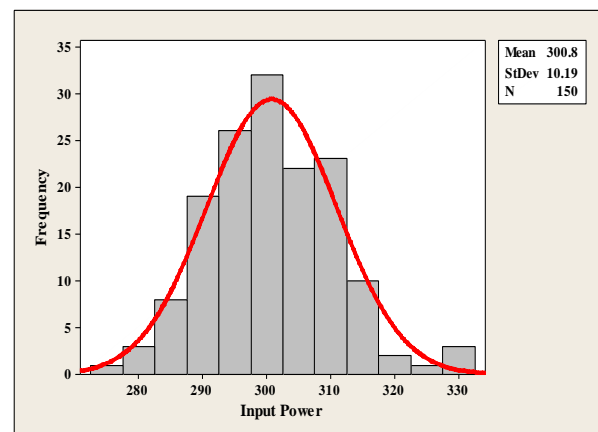


Fig. 8: Distribution of random variables

In this study, both simulations of deterministic and probabilistic analyses were carried out using the process parameters as follows:

Table 1: Thermal cutting parameters

Parameters	Types of analyses	
	Normal (Deterministic)	Monte Carlo (Probabilistic)
Input power, P (W)	300	$\mu = 300W, \sigma = 10$
Cutting speed, v (mm/s)	10	10
Heat source model	3D conical	3D conical

### 3. Results and Discussion

After the simulations were completed, the postprocessing analyses could be implemented in which the temperature distributions caused by the thermal cutting process could be observed. Figure 9 displays the predicted result of temperature distribution at 5 seconds after the cutting process was finished which was at the final time (15s) of simulation. The cutting time was 10 seconds.

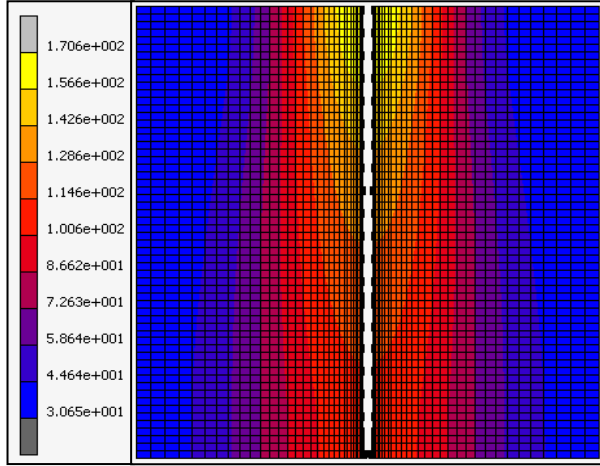


Fig. 9: Temperature distribution after the thermal cutting process was finished (15s).

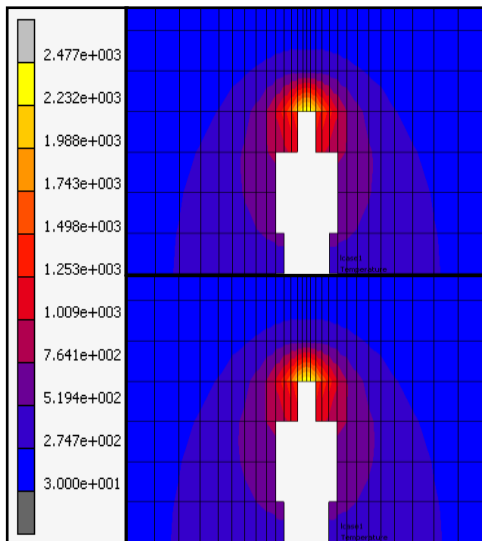


Fig. 10: Comparison of temperature distributions at 5 seconds for the probabilistic (upper) and deterministic (lower) methods.

The temperature distribution as exhibited in Figure 9 represented for both types of analyses since the temperature distribution produced by deterministic method was similar to probabilistic method. Thus, in order to observe the differences in the output results, a comparison of temperature distributions for both analyses had been made by selecting the results a particular time which was at 5 seconds during the cutting proses as shown in Figure 10. Referring to Figure 10, there were slight differences in the contours of temperature distributions between both methods. Therefore, to observe more significant difference in results, one identical node for both cases that is node 9803 was chosen. This node was selected due to its location which is close to the cutting trajectory. Consequently, it would have more significant impact in term of temperature variation as compared to the other nodes farther from the cutting line. The location of the chosen node is shown in Figure 11. In both simulations, the geometrical model was constructed by using 26779 nodes.

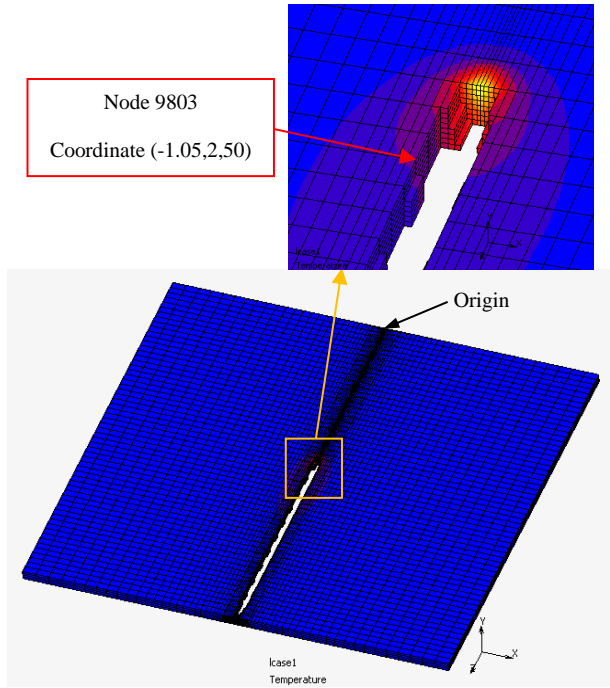


Fig. 11: Location of node 9803

Based on the results at the node, temperature distributions had been plotted in one graph for both cases in order to compare the temperature history from 4.5 seconds up to 5.5 seconds as presented in Figure 12. In the graph, MC and Non MC stand for Monte Carlo and deterministic (without Monte Carlo) methods respectively.

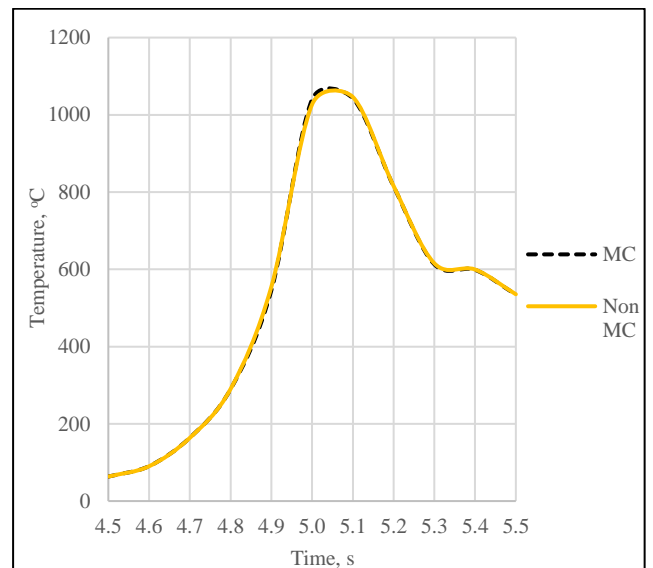


Fig. 12: Temperature distributions at node 9803 between 4.5 and 5.5 seconds.

From the graph above, it could be observed that there were slight differences in temperature distributions between both methods. However, in order to observe better result comparison, the exact values of temperatures at each increment from 4.5 seconds up to 5.5 seconds for both methods were tabulated in Table 2 as follows:

Table 2: Temperature variations at node 9803 between 4.5 and 5.5 seconds

Time (s)	Monte Carlo Probabilistic Temperature (°C)	Normal (Deterministic) Temperature (°C)	Temperature difference  ΔT  (°C)
4.5	63.4256	63.3712	0.0544
4.6	90.4398	90.1612	0.2786

4.7	164.049	163.708	0.3410
4.8	289.593	290.215	0.6220
4.9	545.476	554.477	9.0010
5.0	1039.99	1027.11	12.880
5.1	1042.66	1046.13	3.4700
5.2	814.877	815.895	1.0180
5.3	612.892	615.495	2.6030
5.4	598.513	599.472	0.9590
5.5	534.597	535.445	0.8480

Based on the numerical values of temperatures as presented in the table above, it could be seen that the temperature differences varying between 0.0544 °C and 12.880 °C. The temperature differences proved that the Monte Carlo method produced different results from the deterministic analysis. Hence, this finding could also reflect that the other identical nodes in the both models should have different values of temperature distributions especially at the nodes located near to the cutting trajectory.

#### 4. Conclusions

From the analysis of the results, it was found that slight differences in temperature distributions had been produced between probabilistic and deterministic methods. Even though the differences were not very significant, but more importantly the Monte Carlo method could be implemented successfully and produced different prediction from the normal deterministic analysis. In this research, the Monte Carlo method was just employed to variate the input power while the other parameters were still maintained and thus producing minor changes in the predicted results. More significant difference in results could be obtained through probabilistic method by varying more than one parameter. However, the capability of Monte Carlo method is dependent on the output random numbers. In FEM analysis, there are a lot of random number generators that can be applied to achieve that purpose. The random number generator used in this study was one of the simple generators that could be incorporated into the normal FEM analysis. Therefore, the effectiveness of probabilistic analysis is dependent on the type of random number generator. The probabilistic analysis could be able to produce better prediction due to it could replicate nearly to the real process as compared to the deterministic analysis. In the real process, the supply of input power is normally fluctuated in certain range and quite impossible to maintain it at certain value. Hence, Monte Carlo method is one of the simulation approaches that can be executed to obtain the prediction that is close to the reality.

#### Acknowledgement

The authors would like to express their gratitude to the staff members of the Advanced Manufacturing Technology Excellence Centre (AMTEC) at Faculty of Mechanical Engineering, Universiti Teknologi MARA (UiTM) Malaysia for encouraging this investigation. This research is financially sponsored by Geran Inisiatif Penyelidikan (GIP) UiTM with reference number 600-IRMI/GIP 5/3 (0019/2016).

#### References

- [1] Arttu Laitinen, *Two-Dimensional Simulation of Thermal Cutting of Low Alloyed Steels*, Master of Science Thesis, Tampere University of Technology, (2015).
- [2] Teräslewyjen Terminen Leikkaus, *Metalliteollisuuden Kustannus-Oy*, ISBN 951-817-221-8, ISSN 0357-7368, Tekninen Tiedotus, Helsinki, (1985).
- [3] Hendricks B.R., *Simulation of Plasma Arc Cutting*, M.Sc. Thesis, Faculty of Engineering, Peninsula Teknikon, (1999), pp:1-42.
- [4] Prasad G.V.S., Siores E., Wong W.C.K., "Laser Cutting of Metallic Coated Sheet Steels", *Journal of Materials Processing Technology*, Vol.74, (1998), pp.234-242.
- [5] Anil P. Varkey, Dr. Shajan Kuriakose, Prof. V Narayanan Unni, "Optimization of Edge Quality during CO<sub>2</sub> Laser Cutting of Titanium Alloy", *International Journal of Innovative Research in Advanced Engineering*, Vol.1, (2014), pp.110-117.
- [6] Nyoon K. Y., Nyeoh C. Y., Mohzani Mokhtar, Razi Abdul Rahman, "Finite Element Analysis of Laser Inert Gas Cutting on Inconel 718", *International Journal of Advanced Manufacturing Technology*, Vol.60, (2012), pp.995-1007.
- [7] Serope Kalpakjian, Steven R. Schmid, *Manufacturing Engineering and Technology*, Pearson Education South Asia Pte Ltd, (2014).
- [8] Lidam RN, Yupiter HPM, Redza MR, Rahim MR, Sulaiman MS, Zakaria MY, Tham G, Abas SK, Haruman E and Chau CY, "Simulation Study on Multipass Welding Distortion of Combined Joint Types using Thermo-Elastic-Plastic FEM", *The Journal of Engineering Research*, Vol.9, No.2, (2012), pp.1-16.
- [9] Jonathan G. Mullins and Jens Gunnars, "Effect of Hardening Model on the Weld Residual Stress Field in Pipe Girth Welds", *20th International Conference on Structural Mechanics in Reactor Technology*, Finland, (2009).
- [10] José David Arregui-Mena, Lee Margetts, Paul M. Mummery, "Practical Application of the Stochastic Finite Element Method", *Arch Computat Methods Eng*, (2014). DOI 10.1007/s11831-014-9139-3.
- [11] Der Kiureghian A, Ke J-B, "The Stochastic Finite Element Method in Structural Reliability", *Probab Eng Mech*, Vol.3, (1988), pp.83-91.
- [12] Cassidy MJ, Uzielli M, Tian YH, "Probabilistic Combined Loading Failure Envelopes of a Strip Footing on Spatially Variable Soil", *Comput Geotech*, Vol.49, (2013), pp.191-205.
- [13] Liu WK, Mani A, Belytschko T, "Finite Element Methods in Probabilistic Mechanics", *Probab Eng Mech*, Vol.2, (1987), pp.201-213.
- [14] Miloš Madić, Miroslav Radovanović and Marin Gostimirović, "ANN Modeling of Kerf Taper Angle in CO<sub>2</sub> Laser Cutting and Optimization of Cutting Parameters using Monte Carlo Method", *International Journal of Industrial Engineering Computations*, Vol.6, (2014), pp.1-10.
- [15] C. S. Wu, H. G. Wang and Y. M. ZHANG, "A New Heat Source Model for Keyhole Plasma Arc Welding in FEM Analysis of the Temperature Profile", *Welding Journal*, (2006), pp.284-291.
- [16] Timothy H. Click, Aibing Liu, George A. Kaminski, "Quality of Random Number Generators Significantly Affects Results of Monte Carlo Simulations for Organic and Biological Systems", *Journal of Computational Chemistry*, Vol.32, No.3, (2010), pp.513-524.
- [17] Mark J. Durst, "Using Linear Congruential Generators for Parallel Random Number Generation", *Proceedings of the 1989 Winter Simulation Conference*, (1989), pp:462-466.
- [18] William J. Thistleton, John A. Marsh, Kenric Nelson and Constantino Tsallis, "Generalized Box-Müller Method for Generating q-Gaussian Random Deviates", *IEEE Transactions on Information Theory*, Vol.53, No.12, (2007), pp.4805-4810.
- [19] Adnane Addaim, Driss Gretete and Abdessalam Ait Madi, "Enhanced Box-Muller method for high quality Gaussian random number generation", *Int. J. Computing Science and Mathematics*, Vol.9, No.3, (2018), pp.287-297.
- [20] J. Rodrigues Dias, "A Simple Generalization of the Box-Muller Method for Obtaining a pair of Correlated Standard Normal Variables", *Journal of Statistical Computation and Simulation*, Vol.80, No.9, (2010), pp.953-958.